Progress In Electromagnetics Research, PIER 100, 397–415, 2010

HOMOGENEOUS AND HETEROGENEOUS BREAST PHANTOMS FOR ULTRA-WIDEBAND MICROWAVE IMAGING APPLICATIONS

J. C. Y. Lai, C. B. Soh, E. Gunawan, and K. S. Low

School of Electrical and Electronic Engineering
Nanyang Technological University
50 Nanyang Avenue, Singapore 639798, Singapore

Abstract—The paper discusses fabrication of homogenous and heterogeneous breast phantoms to simulate the dielectric properties of human breast over the microwave frequency range from 0.5 GHz to 13.5 GHz. The breast phantoms have stable mechanical configuration and dielectric properties suitable for microwave imaging experiments particularly ultra-wideband microwave imaging for breast cancer detection.

1. INTRODUCTION

The potential of ultra-wideband (UWB) breast cancer detection has been demonstrated with experiments on simple homogenous breast phantoms [1–3] as well as simulations with anatomically realistic numerical breast phantoms [4–7].

In published experimental studies on UWB for breast cancer detection, soy bean oil is commonly used as the breast phantom material due to easy availability. Apart from soy bean oil, flour-oil-saline mixture [2], corn syrup and glycerin [3] have been used as breast medium in UWB imaging experiments.

However, the materials used as breast phantoms thus far are either having dielectric permittivity much lower than human breast, or the materials are unable to simulate the heterogeneous nature of human breast in solid form. It is necessary to bridge the gap between the simple phantoms that have been used in UWB imaging experimental feasibility studies and the much more complex numerical human breast phantoms in simulation studies.

Corresponding author: C. B. Soh (ecbsoh@ntu.edu.sg).

For building more realistic breast phantom which consists of low-water-content adipose tissues, high-water-content glandular tissues and cancerous lesions, the breast phantom materials are required to have the following features [8]:

- Able to simulate the dielectric properties of human breast over the whole UWB frequencies range (3.1 GHz–10.6 GHz)
- Able to exhibit long-term stable heterogeneity configurations without the risk of their mechanical and electrical properties changing due to diffusion across the interface.

Recently, oil-in-gelatin dispersions with the above requirements have been proposed by Lazebnik et al. [8]. The material consists of an emulsion of oil droplets in gelatin solution which solidifies to a stable material by using liquid surfactant and formalin. By varying the percentage of oil and gelatin, a wide range of dielectric properties can be created. The dielectric properties of the materials are shown to be stable for at least nine weeks after preparation.

The oil-in-gelatin dispersions have been used for ultrasound imaging studies in the past [9]. Anthropomorphic ultrasound breast phantom containing intermediate-sized scatterers has been created successfully [10, 11]. For ultrasound application, the materials are made to mimic the acoustic impedances of the human tissues. For UWB imaging application, the same materials can be used to mimic the dielectric properties of the human tissues.

In [8], only small samples of material are prepared and assessed. The volume of the samples is 20 ml and only the dielectric properties of top surface are measured. This paper attempts to build homogenous and heterogeneous breast phantoms which mimic the dielectric properties of human breast based on the proposed material. Dielectric inconsistency due to the larger volume of breast phantoms is discussed.

2. MATERIALS AND METHODS

Table 1 shows the dielectric permittivity and conductivity of breast phantoms used in the previously reported experimental and simulation studies, as compared to the values of actual human breast reported in literature. Experiments with imaging results are reported by [1] and [2] with low dielectric breast phantoms. For higher dielectric breast phantom, dielectric measurement of the material is reported [12]. Thus far, all the materials used are homogeneous.

In simulation studies, the commonly assumed dielectric permittivity for numerical breast phantom is 9.8 with 10% variability. The values are extrapolated from the three measurement studies on human breast tissues [13–15].

Table 1. Dielectric permittivity and conductivity of breast in experiments, simulations and measurement studies.

Breast Phantoms in Experiments	**Frequency**	**Dielectric Permittivity**	**Conductivity (S/m)**	**Variability**
Xu Li et al. (2004) [1]	6 GHz	2.6	0.05	0%
Fear et al. (2005) [2]	4 GHz	4.2	0.16	0%
Bindu et al. (2004) [12]	3.2 GHz	11.2–44.4	0.66–2.8	0%
Breast Phantoms in Simulations				
Xu Li et al. [4] Fear et al. [5] Yao Xie et al. [7]	6 GHz	8.8–10.8	0.36–0.44	10%
Bond et al. [6]	6 GHz	9.8–33.2	0.4–2.9	10–50%
Human Breasts				
Campbell et al. [16]	3.2 GHz	9.8–46	0.37–3.4	64%
Lazebnik et al. [17]	5 GHz	4.4–48	0.02–4.5	67%

In contrast to the commonly assumed values, two larger scale measurement studies by Campbell et al. [16] and Lazebnik et al. [17] show that the breast dielectric permittivity and conductivity have larger variability. In Table 1, variability is calculated as the range of the dielectric permittivity divided by two times the median.

Therefore, the goal of this paper is to design breast phantoms with dielectric properties more realistic than the previously used experimental and numerical breast phantoms. The design goal of this paper is shown in Table 2 where three homogeneous and seven heterogeneous breast phantoms are fabricated. Since the mean dielectric permittivity of actual human breast is unknown and subject specific, it is assumed to be 8 to 24 in this study.

The range of dielectric permittivity for heterogeneous breast phantoms is calculated from the difference between dielectric permittivity of clutters and matrix materials which will be discussed in Section 2.3.

Table 2. Design goal: three homogeneous and seven heterogeneous breast phantoms.

Breast Phantom	Mean Dielectric Permittivity	Dielectric Permittivity	Range of Dielectric Permittivity	Variability
Homo-80	8	8	0	0%
Homo-65	16	16	0	0%
Homo-50	24	24	0	0%
Hetero-17	10	8–24	16	±80%
Hetero-25	11	8–24	16	±73%
Hetero-33	13	8–24	16	±62%
Hetero-50	16	8–24	16	±50%
Hetero-60	13	8–20	12	±46%
Hetero-65	11	8–16	8	±36%
Hetero-70	10	8–12	4	±20%

2.1. Production of Tissue-mimicking Phantom Materials

Phantom materials of different content of oil and water were produced in cylindrical polypropylene containers with dimension of 5 cm height and 10 cm diameter, according to the method presented by Lazebnik et al. [8]. The volume of each material was 400 ml which fully occupied the container. The materials were properly sealed to prevent desiccation. Six samples were produced with 10%, 30%, 50%, 60%, 70% and 80% of oil.

2.2. Fabrication of Homogeneous Breast Phantoms

Breast phantoms were fabricated in cylindrical polypropylene containers with dimension of 8 cm height and 10 cm diameter. Three homogeneous breast phantoms were fabricated with 50%, 65%, and 80% of oil. Breast phantoms were fabricated with volume of 600 ml to fully occupy the polypropylene containers. The breast phantoms were turned top-to-bottom every half an hour for the next 6 hours after fabrication. The procedure is to avoid water migration towards the bottom of the phantom.

2.3. Fabrication of Heterogeneous Breast Phantoms

Seven heterogeneous breast phantoms were fabricated by mixing phantom materials made of different volume of oil. Clutters were

made of material with low percentage of oil to simulate the glandular tissue, whereas matrix to hold the clutters was made of materials with high percentage of oil to simulate the adipose tissue in human breast. Clutters were prepared by mincing the high dielectric phantom material to size smaller than 5 mm.

A thin layer of matrix material (80% oil) was first poured into the phantom container. A thin layer of clutter material (50% oil) was then deposited on the thin layer of matrix material. Another thin layer of matrix material was poured onto the thin layer of clutter material to just cover the clutters as shown in Figure 1. The process was repeated until the phantom materials fully filled the container.

Phantoms Hetero-17, Hetero-25, Hetero-33, and Hetero-50 were fabricated by fixing the clutters dielectric permittivity and varying the percentage of clutters to simulate different volumes of glandular and fibroconnective tissues. Phantoms Hetero-70, Hetero-65, and Hetero-60 were fabricated by fixing percentage of clutters and varying the clutters dielectric permittivity to simulate different breast dielectric properties. The compositions of different breast phantoms are shown in Table 3.

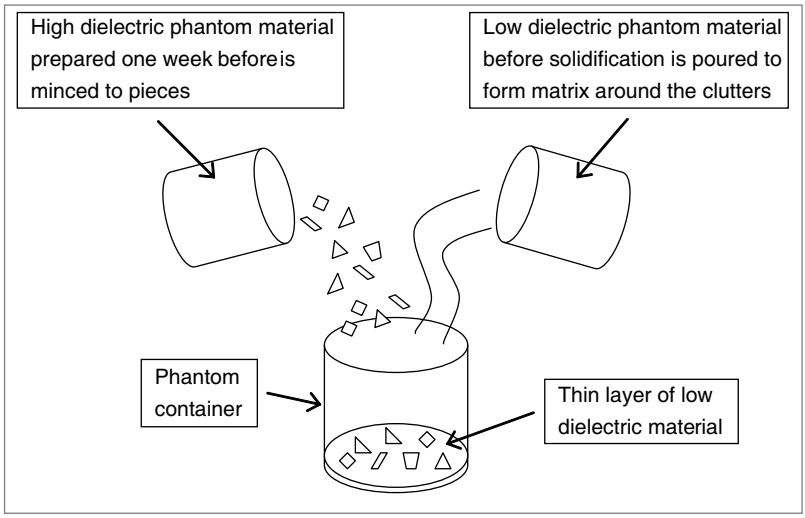

Figure 1. High dielectric clutter material (left) and low dielectric matrix material (right) are mixed during fabrication of heterogeneous breast phantom.

Table 3. Compositions of seven heterogeneous breast phantoms.

Phantom	Volume % of oil in clutters	Volume % of clutters in phantom	Volume % of oil in phantom
Hetero-17	50%	17%	75%
Hetero-25	50%	25%	73%
Hetero-33	50%	33%	70%
Hetero-50	50%	50%	65%
Hetero-70	70%	50%	75%
Hetero-65	65%	50%	73%
Hetero-60	60%	50%	70%

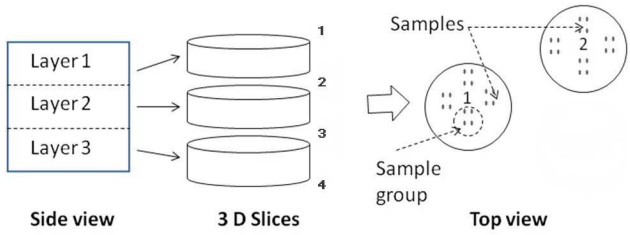

Figure 2. Description of dielectric measurement procedure.

2.4. Dielectric Properties Measurement

Dielectric measurements were conducted one week after the fabrication when the phantoms had solidified. Measurements, with frequencies range from 0.5 GHz to 13.5 GHz, were conducted using Agilent N5230A vector network analyzer and Agilent 85070 slim-formed open-ended coaxial probe. Reflection coefficients were converted to dielectric permittivity and loss tangent by Agilent 85070 dielectric measurement software. The measurement accuracy and repeatability specified by the manufacturer is 5% and 1.5% respectively. The probe accuracy and repeatability had been verified using methanol, ethanol, and propanol.

In order to analyze the dielectric consistency of phantom material, the material was sliced into three layers consisting of four surfaces as shown in Figure 2. For each surface, sixteen measurements were taken from four sample groups with each group of measurements taken from a circular region of 1 cm radius. As such, a total of 64 measurements were collected from each phantom.

After measuring each sample group, the probe was cleaned with tissue paper to prevent any oil that may accumulate on it during measurements. After cleaning, measurement of air was taken to ensure that the dielectric permittivity does not drift away from 1.

Probe calibration was conducted after every sixteen measurements (one surface) to ensure accuracy.

The homogeneity of the phantom material was assessed by comparing the dielectric properties between different regions within the same surface, and between different surfaces within the same phantom. The dielectric permittivity and conductivity are plotted in Figure 3 with different color for each surface. From bottom surface to top surface, the color representations are red, magenta, blue, and cyan.

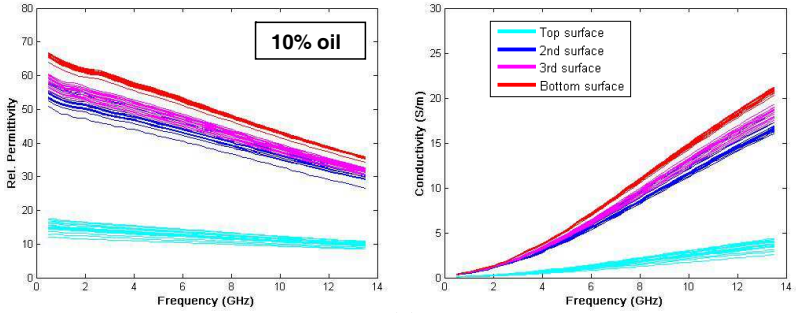

(a)

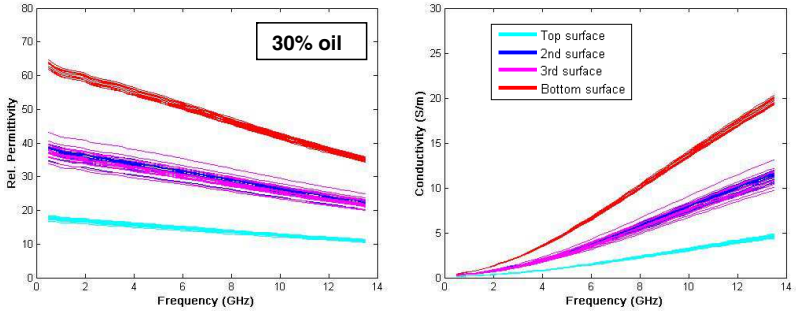

(b)

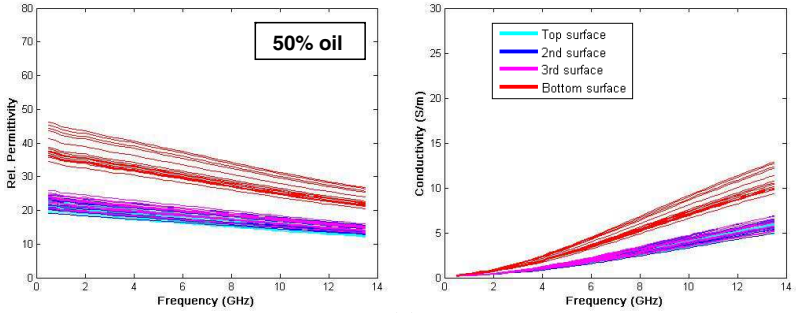

(c)

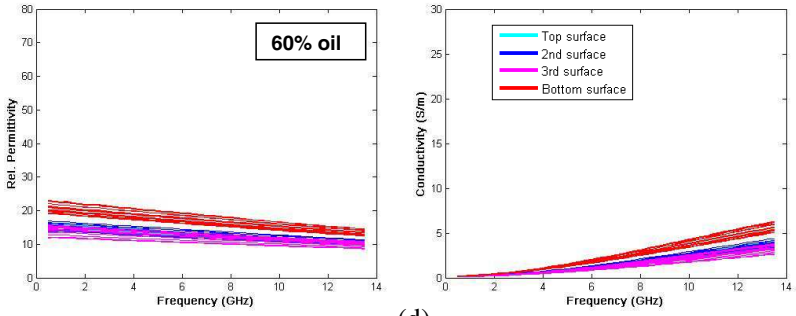

(d)

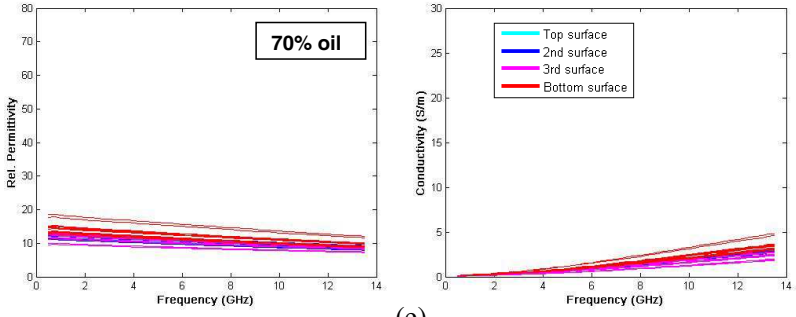

(e)

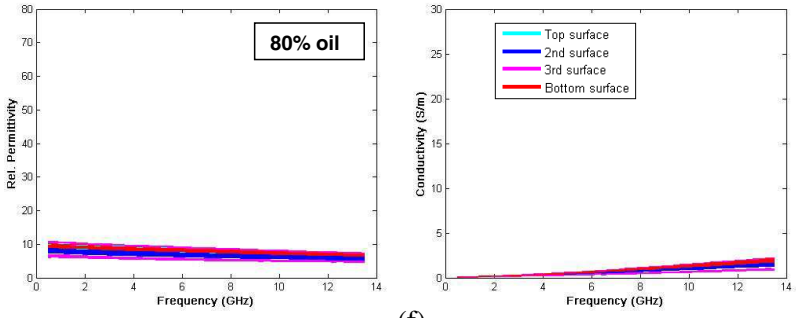

(f)

Figure 3. (a) Dielectric permittivity and conductivity of material with 10% of oil. (b) Dielectric permittivity and conductivity of material with 30% of oil. (c) Dielectric permittivity and conductivity of material with 50% of oil. (d) Dielectric permittivity and conductivity of material with 60% of oil. (e) Dielectric permittivity and conductivity of material with 70% of oil. (f) Dielectric permittivity and conductivity of material with 80% of oil.

For homogeneous and heterogeneous breast phantoms, the phantom was sliced into seven layers consisting of eight surfaces. A total of 128 measurements were collected similar to the procedure mentioned above.

3. RESULTS AND DISCUSSION

3.1. Tissue-mimicking Phantom Materials

Figure 3 shows that there is large inconsistency in dielectric permittivity for different surfaces within a phantom material which is undesirable. The surface-to-surface dielectric constants vary greatly for phantom materials with low percentages of oil which is quantified as the phantom variability in Table 4. This is caused by migration of water over time towards the bottom of the phantom due to gravity before solidification of the materials which occurs one week after fabrication. The dielectric permittivity of the bottom surface tends to be higher due to the concentration of water and the dielectric permittivity of the top surface tends to be lower due to loss of water.

However, there is no significant difference for dielectric permittivity at different regions on the same surface. Although the materials are not suitable to be used as breast phantoms as a whole, breast tissues of different dielectric properties can be simulated by using the materials from the middle layers. Further, the higher percentage oil materials do not show significant inconsistencies, and so can be useable as homogeneous high-adipose-tissue breast phantoms. Considering only the middle layers, the dielectric permittivity and conductivity of the samples are in agreement with the samples prepared by Lazebnik et al. [8].

Table 4. Variability and mean of different groups measurements for phantom materials.

Material	1 cm radius circular region	Surface	Phantom	Mean
10% oil	5.5%	5.9%	80.9%	40.58
30% oil	6.1%	7.6%	81.9%	33.08
50% oil	10.5%	16.7%	57.2%	22.52
60% oil	9.7%	12.2%	33.5%	14.63
65% oil	11.5%	18.0%	26.9%	12.88
70% oil	12.6%	16.4%	21.2%	11.31
80% oil	7.3%	24.2%	27.3%	7.72

3.2. Homogeneous Breast Phantoms

Measurement results for dielectric permittivity at 5 GHz are shown with box plots and histograms in Figures 4 to 6. All the analysis is conducted only for dielectric permittivity at 5 GHz. This is because the variability of dielectric permittivity is approximately linear across the frequency range of measurement (0.5 GHz to 13.5 GHz) as can be seen in Figure 3. Analysis of variance (ANOVA) is conducted to analyze the layer-to-layer difference of homogeneous breast phantoms.

Results in Figures 4 to 6 show that turning the phantoms top-to-bottom and bottom-to-top does not totally resolve the water migration problem. However if the top and bottom layers are excluded from analysis, the layer-to-layer difference is not significant.

When considering the six layers in the middle part of phantoms, ANOVA results are between 0.013 and 0.91, whereas when considering

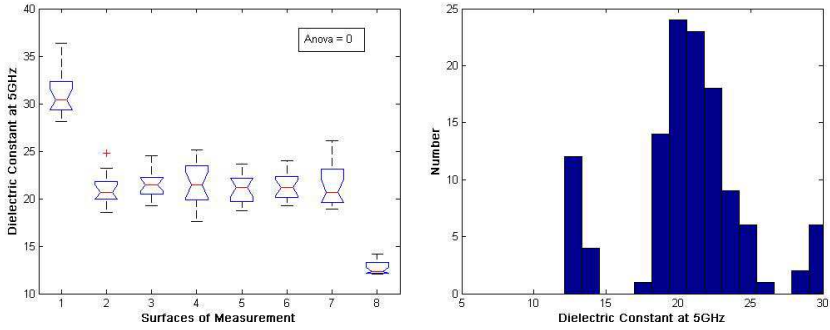

Figure 4. Breast phantom Homo-50. Box plot (left) for 8 surfaces measurements. Histogram (right) of 128 measurements.

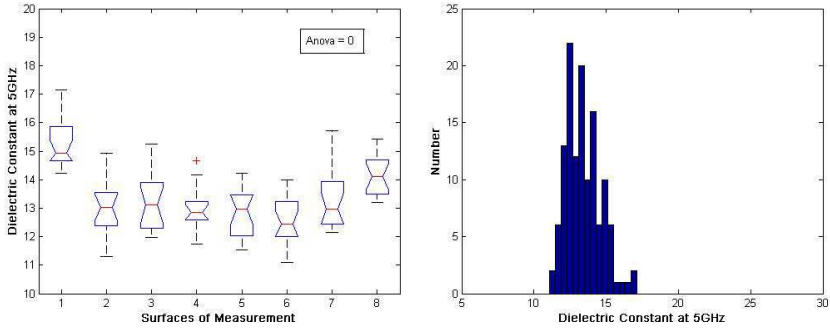

Figure 5. Breast phantom Homo-65. Box plot (left) for 8 surfaces measurements. Histogram (right) of 128 measurements.

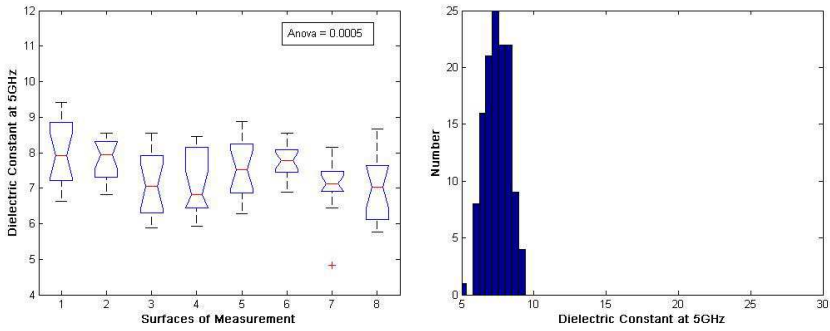

Figure 6. Breast phantom Homo-80. Box plot (left) for 8 surfaces measurements. Histogram (right) of 128 measurements.

all layers, ANOVA results are smaller than 0.0005 showing that the top and bottom layers are significantly different from the middle layers. For UWB imaging, the top and bottom layers can be excluded by chopping the breast phantom after fabrication to obtain a more homogeneous phantom.

Histograms of dielectric permittivity at 5 GHz are plotted at right side of Figures 4 to 6. Results show that the breast phantom with higher dielectric permittivity has larger variability.

3.3. Heterogeneous Breast Phantoms

Measurement results for dielectric permittivity at 5 GHz are shown with box plots and histograms in Figures 7 to 13.

The distributions of the dielectric constants are skewed to the left. The distribution skewness is higher for breast phantom with lower volume percentage of clutters of the same dielectric permittivity. This is because the dielectric measurements are conducted with random selection of samples. In most of the instances, the probe is measuring the matrix, and in few instances the probe is measuring the clutter.

The distributions show that the variability of the dielectric properties in breast tissues can be successfully simulated with clutters of single dielectric permittivity. By mincing the phantom material to small size (< 5 mm), the distinct dielectric permittivity of small clutters will be averaged with the surrounding low dielectric matrix medium. This is because the small clutters are considered microscopic at microwave frequencies. Thus a smooth distribution from low to high dielectric permittivity can be created to represent the breast dielectric variability.

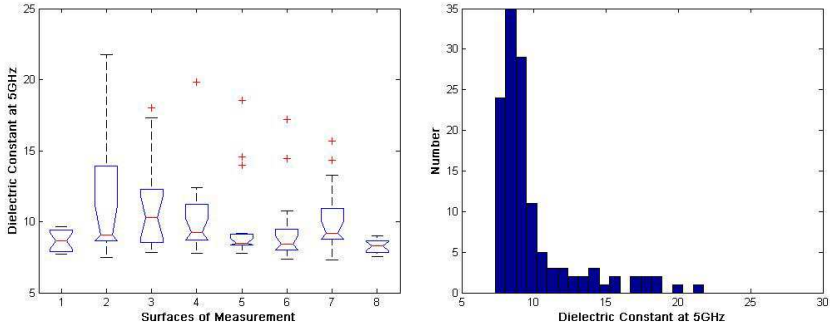

Figure 7. Breast phantom Hetero-17. Box plot (left) for 8 surfaces measurements. Histogram (right) of 128 measurements.

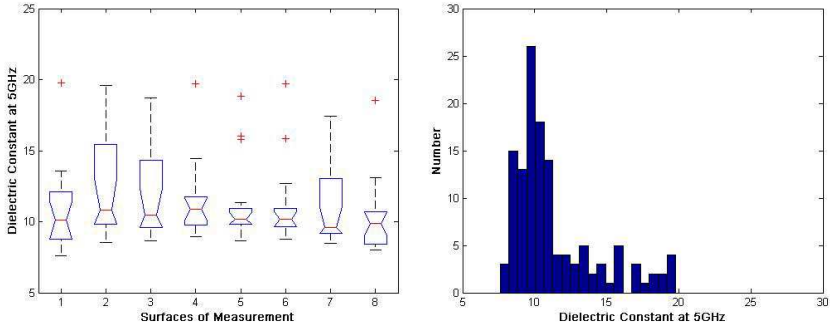

Figure 8. Breast phantom Hetero-25. Box plot (left) for 8 surfaces measurements. Histogram (right) of 128 measurements.

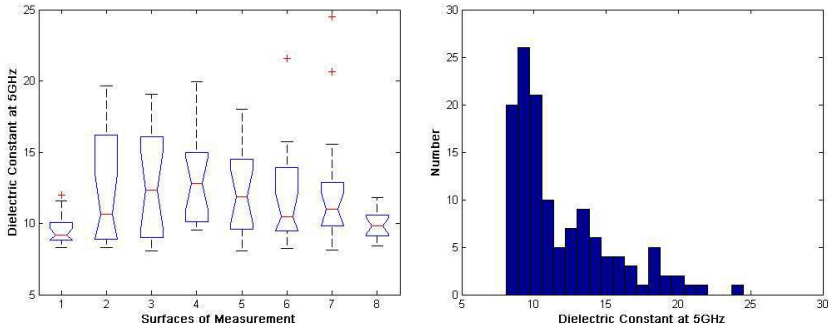

Figure 9. Breast phantom Hetero-33. Box plot (left) for 8 surfaces measurements. Histogram (right) of 128 measurements.

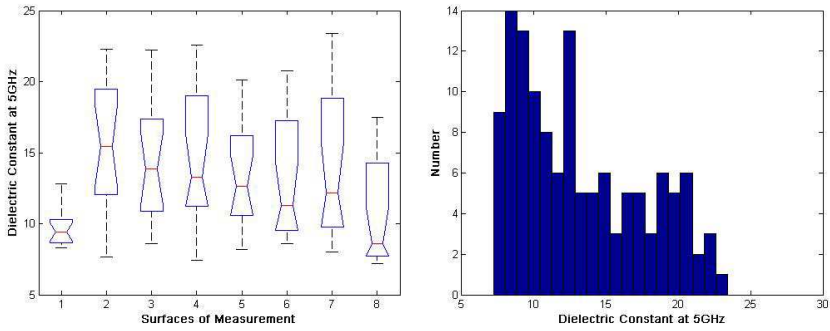

Figure 10. Breast phantom Hetero-50. Box plot (left) for 8 surfaces measurements. Histogram (right) of 128 measurements.

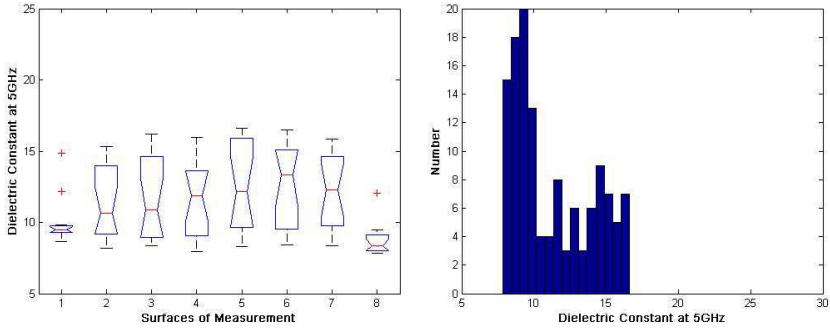

Figure 11. Breast phantom Hetero-60. Box plot (left) for 8 surfaces measurements. Histogram (right) of 128 measurements.

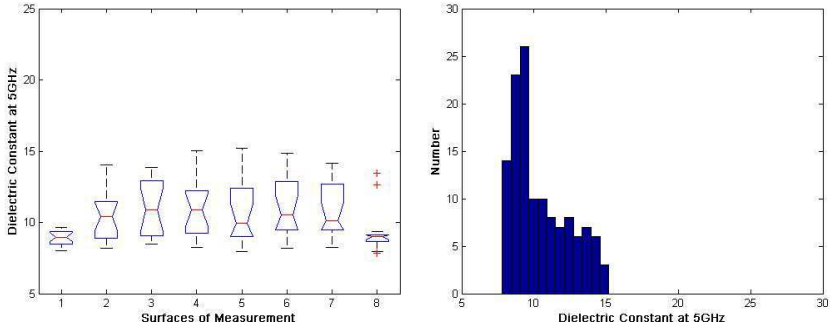

Figure 12. Breast phantom Hetero-65. Box plot (left) for 8 surfaces measurements. Histogram (right) of 128 measurements.

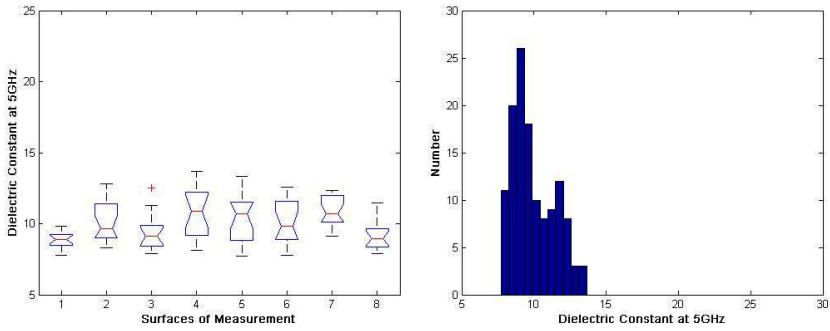

Figure 13. Breast phantom Hetero-70. Box plot (left) for 8 surfaces measurements. Histogram (right) of 128 measurements.

The dielectric permittivity of the top and bottom layers is low because the clutters are totally covered by the matrix material. During the fabrication process, a thin layer of matrix material is first poured at the bottom of the phantom and finally the top of the phantom is covered with a thin layer of matrix material.

3.4. Analysis of Dielectric Variability

Analysis of dielectric variability was conducted by comparing the variability of different measurement groups within a phantom. Variability is calculated as 2 times the standard deviation divided by mean. For phantom materials, variability are calculated for 4 samples from the same circular region of 1 cm radius, 16 samples for each surface, and a total of 64 samples for each phantom.

Results in Table 4 show that variability for each phantom is large for phantom materials with lower concentration of oil. The results are expected due to the large layer-to-layer differences as shown in Figure 3. The variability of 1 cm radius circular region and same surface are smaller than 25%, showing that the dielectric permittivities for each layer are relatively consistent.

There is improvement for the layer-to-layer consistency with the fabrication procedure used in homogeneous breast phantom as compared to phantom materials as shown in Table 5. By excluding the top and bottom layers of the breast phantoms, the phantom variability becomes smaller, showing that the dielectric constants of the middle parts of phantoms are consistent and are suitable as breast phantoms for microwave imaging experiments.

Table 5. Variability and mean of homogeneous breast phantoms.

Phantom	1 cm radius circular region	Surface	Phantom	Mean
Homo-50	15.5%	16.7%	46.2%	21.44
Homo-65	10.1%	13.4%	17.9%	13.42
Homo-80	15.2%	21.5%	23.3%	7.44
Top and bottom layers excluded				
Homo-50	17.5%	16.6%	16.3%	21.27
Homo-65	11.3%	14.3%	14.4%	12.99
Homo-80	15.5%	20.0%	21.2%	7.42

Table 6. Variability and mean of heterogeneous breast phantoms.

Phantom	1 cm radius circular region	Surface	Phantom	Mean
Hetero-17	55.8%	56.2%	58.4%	9.86
Hetero-25	51.8%	52.9%	52.6%	11.32
Hetero-33	57.1%	55.8%	58.4%	11.85
Hetero-50	63.6%	62.1%	66.5%	13.23
Hetero-60	46.2%	44.3%	48.3%	11.28
Hetero-65	34.9%	35.7%	37.3%	10.45
Hetero-70	26.7%	27.0%	29.9%	9.97

Table 6 shows the variability of different measurement groups for heterogeneous breast phantoms. There is no significant difference for variability of 1 cm radius circular region, surface, and phantom showing that the clutters are well distributed during fabrication.

For overall results, the dielectric variability for homogeneous breast phantom is below 25% and above 25% for heterogeneous breast phantom. Results show that the fabricated heterogeneous breast phantoms provide the required variability of human breast, which is 67% as shown in Table 1, and thus suitable for microwave imaging experiments.

3.5. Microwave Imaging Experiment

A simple microwave imaging experiment was conducted to show the usefulness of fabricated breast phantom. Breast phantom was placed on a rotary stage with bistatic UWB antennas scanning at the side of phantom container to simulate the human breast in prone position.

Breast phantom was rotated for 360 degrees relative to the stationary antennas to simulate a circular array of 360 antennas around the breast circumference as shown in Figure 14.

The collected signals were processed with confocal imaging technique [4, 5] to generate the breast image. Cross-sectional image of the cylindrical breast phantom was formed by synthetically focusing the signals received from the antenna array to every point within the scanning plane. A tumor of 4 mm made of phantom material with 10% oil was inserted into the breast phantoms at depth of 4 cm from top and 2 cm from the central axis. Two scans were performed for the breast phantom, one with tumor inserted and one without the tumor.

Imaging result of breast phantom Hetero-60 is given in Figure 15. The left figure is obtained from the original breast phantom without tumor inserted. Clutters are visible on the breast image. Although clutters were uniformly distributed in the phantom during fabrication, the image shows that the clutters are concentrated at the center of the phantom. This is because of the simple algorithm used in image construction which produces non-uniform gain for pixel intensities at different radius. The right figure is obtained from breast phantom with tumor inserted showing that the tumor is clearly visible at location 2 cm from the center.

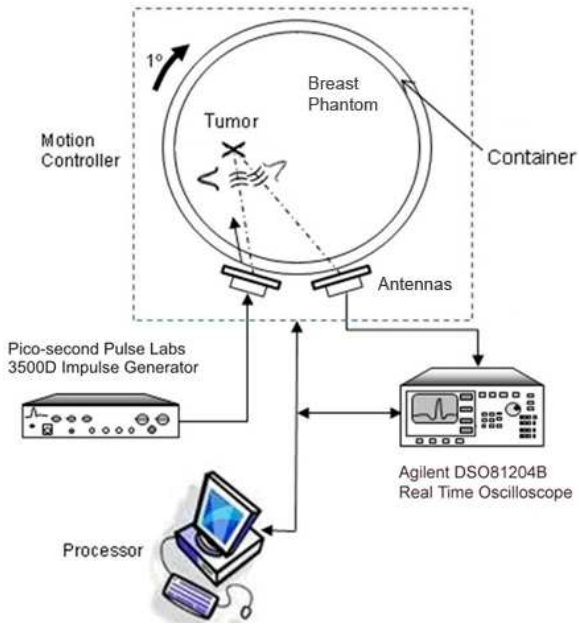

Figure 14. Overall experimental setup.

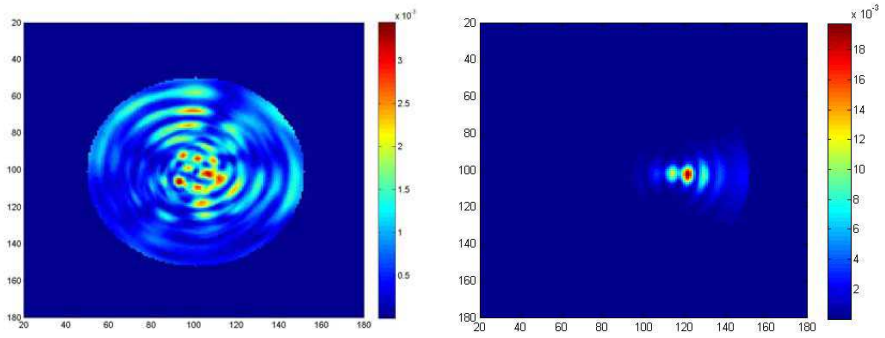

Figure 15. Imaging result of phantom Hetero-60. Left: phantom without tumor showing the presence of clutters. Right: phantom with 4 mm tumor at location (120, 100).

Experiments on the use of the breast phantoms to investigate the performance breast cancer detection algorithms will be the focus of future work.

4. CONCLUSIONS

Homogeneous and heterogeneous breast phantoms were successfully fabricated with oil-in-gelatin dispersion materials. Dielectric measurement results show that the phantoms are able to represent the dielectric properties and variability of human breast in a more realistic manner than the previously reported breast phantoms. The breast phantoms are useful for future microwave imaging experiments.

REFERENCES

1. Li, X., S. K. Davis, S. C. Hagness, D. W. Van Der Weide, and B. D. Van Veen, "Microwave imaging via space-time beamforming: Experimental investigation of tumor detection in multi-layer breast phantoms," *IEEE Transactions on Microwave Theory and Techniques*, Vol. 52, No. 8, 1856–1865, Aug. 2004.
2. Sill, J. M. and E. C. Fear, "Tissue sensing adaptive radar for breast cancer detection — Experimental investigation of simple tumor models," *IEEE Transactions on Microwave Theory and Techniques*, Vol. 53, No. 11, 3312–3319, Nov. 2005.
3. Bindu, G., S. J. Abraham, A. Lonappan, V. Thomas, C. K. Aanandan, and K. T. Mathew, "Active microwave

imaging for breast cancer detection," *Progress In Electromagnetics Research*, PIER 58, 149–169, 2006.

4. Li, X. and S. C. Hagness, "A confocal microwave imaging algorithm for breast cancer detection," *IEEE Microwave and Wireless Components Letters*, Vol. 11, No. 3, 130–132, Mar. 2001.
5. Fear, E. C., X. Li, S. C. Hagness, and M. A. Stuchly, "Confocal microwave imaging for breast cancer detection: Localization of tumors in three dimensions," *IEEE Transactions on Biomedical Engineering*, Vol. 49, No. 8, 812–822, Aug. 2002.
6. Bond, E. J., X. Li, S. C. Hagness, and B. D. Van Veen, "Microwave imaging via space-time beamforming for early detection of breast cancer," *IEEE Transactions on Antennas and Propagation*, Vol. 51, No. 8, 1690–1705, Aug. 2003.
7. Xie, Y., B. Guo, L. Xu, J. Li, and P. Stoica, "Multistatic adaptive microwave imaging for early breast cancer detection," *IEEE Transactions on Biomedical Engineering*, Vol. 53, No. 8, 1647–1657, Aug. 2006.
8. Lazebnik, M., E. L. Madsen, G. R. Frank, and S. C. Hagness, "Tissue-mimicking phantom materials for narrowband and ultrawideband microwave applications," *Physics in Medicine and Biology*, Vol. 50, 4245–4258, 2005.
9. Madsen, E. L., J. A. Zagzebski, and G. R. Frank, "Oil-in-gelatin dispersions for use as ultrasonically tissue-mimicking materials," *Ultrasound in Medicine and Biology*, Vol. 8, 277–287, 1982.
10. Madsen, E. L., J. A. Zagzebski, G. R. Frank, J. F. Greenleaf, and P. L. Carson, "Anthropomorphic breast phantoms for assessing ultrasonic imaging system performance and for training ultrasonographers," *Journal of Clinical Ultrasound*, Vol. 10, 67–75, 1982.
11. Madsen, E. L., J. A. Zagzebski, and G. R. Frank, "An anthropomorphic ultrasound breast phantom containing intermediate-sized scatteres," *Ultrasound in Medicine and Biology*, Vol. 8, 381–392, 1982.
12. Bindu, G., A. Lonappan, V. Thomas, V. Hamsakkutty, C. K. Aanandan, and K. T. Mathew, "Microwave characterization of breast-phantom materials," *Microwave and Optical Technology Letters*, Vol. 43, No. 6, 506–508, 2004.
13. Chaudhary, S. S., R. K. Mishra, A. Swarup, and J. M. Thomas, "Dielectric properties of normal and malignant human breast tissues at radiowave and microwave frequencies," *Indian Journal of Biochemistry & Biophysics*, Vol. 21, 76–79, 1984.

14. Surowiec, A. J., S. S. Stuchly, J. R. Barr, and A. Swarup, "Dielectric properties of breast carcinoma and the surrounding tissues," *IEEE Transactions on Biomedical Engineering*, Vol. 35, No. 4, 257–263, 1988.
15. Joines, W. T., Y. Z. Dhenxing, and R. L. Jirtle, "The measured electrical properties of normal and malignant human tissues from 50 to 900 MHz," *Medical Physics*, Vol. 21, 547–550, 1994.
16. Campbell, A. M. and D. V. Land, "Dielectric properties of female human breast tissue measured in vitro at 3.2 GHz," *Physics in Medicine and Biology*, Vol. 37, 193–210, 1992.
17. Lazebnik, M., L. McCartney, D. Popovic, C. B. Watkins, M. J. Lindstrom, J. Harter, S. Sewall, A. Magliocco, J. H. Booske, M. Okoniewski, and S. C. Hagness, "A large-scale study of the ultrawideband microwave dielectric properties of normal breast tissue obtained from reduction surgeries," *Physics in Medicine and Biology*, Vol. 52, 2637–2656, May 2007.